Available online at www.sciencedirect.com
ScienceDirect
Biochimica et Biophysica Acta 1777 (2008) 250–259
Biochimica et Biophysica Acta
BBA
www.elsevier.com/locate/bbabio

Electron transfer kinetics between soluble modules of *Paracoccus denitrificans* cytochrome c_1 and its physiological redox partners

Julia Janzon [a], Anna Carina Eichhorn [a], Bernd Ludwig [a,b], Francesco Malatesta [c,*]

[a] *Molecular Genetics Group, Institute of Biochemistry, Biocentre J. W. Goethe-University Frankfurt/Main, Germany*
[b] *Cluster of Excellence "Macromolecular Complexes", Frankfurt/Main, Germany*
[c] *Department of Pure and Applied Biology, University of L'Aquila, L'Aquila, Italy*

Received 17 July 2007; received in revised form 7 January 2008; accepted 9 January 2008
Available online 16 January 2008

Abstract

The transient electron transfer (ET) interactions between cytochrome c_1 of the bc_1-complex from *Paracoccus denitrificans* and its physiological redox partners cytochrome c_{552} and cytochrome c_{550} have been characterized functionally by stopped-flow spectroscopy. Two different soluble fragments of cytochrome c_1 were generated and used together with a soluble cytochrome c_{552} module as a model system for interprotein ET reactions. Both c_1 fragments lack the membrane anchor; the c_1 core fragment (c_{1CF}) consists of only the hydrophilic heme-carrying domain, whereas the c_1 acidic fragment (c_{1AF}) additionally contains the acidic domain unique to *P. denitrificans*. In order to determine the ionic strength dependencies of the ET rate constants, an optimized stopped-flow protocol was developed to overcome problems of spectral overlap, heme autoxidation and the prevalent non-pseudo first order conditions. Cytochrome c_1 reveals fast bimolecular rate constants (10^7 to 10^8 M^{-1} s^{-1}) for the ET reaction with its physiological substrates c_{552} and c_{550}, thus approaching the limit of a diffusion-controlled process, with 2 to 3 effective charges of opposite sign contributing to these interactions. No direct involvement of the N-terminal acidic c_1-domain in electrostatically attracting its substrates could be detected. However, a slight preference for cytochrome c_{550} over c_{552} reacting with cyochrome c_1 was found and attributed to the different functions of both cytochromes in the respiratory chain of *P. denitrificans*.

Keywords: Cytochrome bc_1; Cytochrome c_1 soluble modules; Electron transfer; *Paracoccus denitrificans*

1. Introduction

The cytochrome bc_1-complex (ubiquinol: cytochrome *c* reductase, EC 1.10.2.2) is an essential component of the respiratory chain of prokaryotes and eukaryotes [1,2]. As a multisubunit integral membrane metalloprotein it catalyzes electron transfer (ET) from ubiquinol to cytochrome *c*. This reaction is coupled to proton translocation across the membrane by the Q-cycle mechanism [3–7] and the generated electrochemical gradient is used by the ATP synthase to drive ADP phosphorylation. X-ray structures of several bc_1-complexes have been solved [1,8–12] and allow insight into their structural composition and funtional aspects. While bc_1-complexes of eukaryotes consist of up to 11 different subunits, the composition of prokaryotic bc_1-complexes is much simpler and restricted to the essential catalytic polypeptides. The bc_1-complex of the gram-negative, metabolically flexible soil bacterium *Paracoccus denitrificans* comprises solely the three redox-active subunits encoded in the *fbc*FBC-operon [13]. Its Rieske iron sulfur protein (ISP) consists of 190 amino acids and carries a [2Fe–2S] cluster. *Fbc*B encodes cytochrome *b*, a 440 amino acid polypeptide housing hemes b_L and b_H. Cytochrome c_1, the *fbc*C gene product, is a polypeptide of 450 amino acids carrying a covalently attached *c*-type heme. According to hydrophathy and sequence analysis

Abbreviations: c_{1CF}, soluble cytochrome c_1 core fragment from *Paracoccus denitrificans*; c_{1AF}, soluble cytochrome c_1 acidic fragment from *Paracoccus denitrificans*; c_{552F}, soluble cytochrome c_{552} fragment from *Paracoccus denitrificans*; c_{550}, soluble cytochrome c_{550} from *Paracoccus denitrificans*; c_{hh}, horse heart cytochrome *c*; c_{551Pa}, cytochrome c_{551} from *Pseudomonas aeruginosa*; ET, electron transfer

* Corresponding author. Department of Pure and Applied Biology, University of L'Aquila, via Vetoio-loc. Coppito, I-67010 L'Aquila, Italy. Tel.: +39 0862433287; fax: +39 0862433273.
E-mail address: malatest@univaq.it (F. Malatesta).

0005-2728/$ - see front matter © 2008 Elsevier B.V. All rights reserved.
doi:10.1016/j.bbabio.2008.01.003

[13] cytochrome c_1 exhibits a tripartite domain structure: a C-terminal membrane anchor, a periplasmically oriented core domain liganding the *c*-type heme group, and a unique N-terminal, acidic domain of 150 amino acids showing a remarkable amino acid composition, with around 40% acidic residues, 40% alanines and 18% prolines, lacking any basic amino acids [13,14]. It is thus reminiscent of the small acidic subunits of eukaryotic bc_1-complexes associated with the c_1 subunits [15–18] such as the hinge protein of the bovine bc_1-complex [19] or subunit 6 of the yeast complex [11], which are proposed to participate in the interaction between cytochrome c_1 and cytochrome *c* due to their highly negative surface charge [20,21].

Cytochrome c_{552} is the genuine electron mediator between the bc_1-complex and cytochrome aa_3-oxidase as demonstrated by functional studies using anti-c_{552} antibodies or c_{552} deletion strains to block ET between complex III and IV [22]. Under certain solubilization conditions supercomplexes containing cytochrome c_{552}, the bc_1-complex and cytochrome *c* oxidase [23,24] as well as complex I [25] could be isolated showing high ET rates. The *cyc*M gene coding for cytochrome c_{552} has been cloned and sequenced [22]. Cytochrome c_{552} is a 176 amino acid membrane-bound *c*-type cytochrome also comprising a tripartite domain structure derived from sequence analysis [22]: The N-terminal membrane anchor is followed by a hydrophilic, flexible, negatively charged linker region and a C-terminal, hydrophilic domain housing the covalently attached heme. The latter domain of 100 amino acids has been cloned and expressed in *E. coli* [26]. Its three-dimensional structure has been solved by X-ray crystallography [27] as well as multi-dimensional heteronuclear NMR spectroscopy [28–30] for both redox states, and its interactions with the soluble Cu_A-fragment of cytochrome aa_3-oxidase have been studied [31]. Even though it has a slightly acidic isoelectric point, it closely resembles the mitochondrial cytochrome *c* in its overall structure and surface charge distribution around the heme crevice, where a total of 9 lysine residues are thought to mainly govern the interaction with cytochrome *c*-oxidase [32].

An alternative electron acceptor of the *P. denitrificans* bc_1-complex is the soluble cytochrome c_{550} functioning as electron mediator in several respiratory pathways such as denitrification [33,34], methanol and methylamine oxidation [35,36] and acting as electron donor for the cbb_3-and aa_3-oxidases [37].

In the study of transient interactions of redox proteins functional approaches have been undertaken in the past revealing a strong electrostatic component [38]. In the cytochrome c_1/cytochrome *c* couple, conserved lysine residues surrounding the heme crevice of cytochrome *c* interacting with acidic residues of cytochrome c_1 were identified [21,39–42]. Soluble fragments of redox proteins have been used successfully to characterize ET reactions between redox partners [32,43–47]. In contrast to this, structural determinations of different redox complexes revealed small compact contact sites, where direct contacts are mainly mediated by hydrophobic interactions [31,48–50]. The reaction interfaces of transient electron transfer complexes, including *P. denitrificans* amicyanin-cytochrome c_{551} [51,52] and amicyanin:methylamine-dehydrogenase [53] as well as yeast bc_1:cytochrome *c* [39,50], cytochrome *c*-peroxidase:cytochrome *c* [48,54] and *Rhodobacter* cytochrome c_2:reaction center [49,55], have been described by functional, structural and computational studies [56] showing a small contact site of low atomic packing, mainly consisting of apolar residues engaging in direct hydrophobic contacts. This area is surrounded by patches of charged residues at the periphery – complementary charged for interacting redox partners – which are responsible for fast electrostatic association and pre-orientation of the redox partners yielding an encounter complex, followed by hydrophobic fine tuning yielding the active ET-complex.

Here we report a functional approach to determine the transient ET interactions of cytochrome c_1 of the bc_1-complex of *P. denitrificans* with its physiological redox partners using soluble fragments as a model system. We show that the ET reaction yields very fast apparent bimolecular rate constants (10^7 to 10^8 $M^{-1}s^{-1}$) and approaches the limit of a diffusion-controlled process, with 2 to 3 charges contributing to the interaction.

2. Materials and methods

2.1. Cloning, expression and purification procedures

In order to clone the soluble cytochrome c_1 core (c_{1CF}) and the acidic fragments (c_{1AF}), the complete *fbc* operon was subcloned into StuI/NcoI restricted pSelect. The *fbc* operon from *Paracoccus denitrificans* is depicted in Fig. 1 along with the translation products used in this study. After digestion with SfiI/HindIII a 3515 bp fragment was obtained from the pSelect construct that served as template for the subsequent PCR, which introduced a restriction site for NcoI and HindIII using the following primers (mutagenic sequences in bold) cytc_1_HindIII: 5′-CAC CGA GAC GAA **AGG CTT** TCA CTT GCG ATC CAT CAT CTT-3′, cytc_1(c_{1CF})_NcoI:5′-ACG AAG CCG **CCA TGG** ATC ATG GCG ACG CGG CCC GCT C-3′ and cytc_1(c_{1AF})_NcoI: 5′-CAG GCG GCG CCC CAA TGG ACG CAA GCA CCG CGC CCG GCA CGA CG-3′.

The amplified PCR fragments – 669 bp (c_{1CF}) and 1170 bp (c_{1AF}) – were cloned via NcoI/HindIII into pET-22b(+) (Novagen), a T7-based IPTG-inducible expression plasmid specifying the *pel*B-leader signal sequence for direction of the apoprotein to the periplasm for heme incorporation.

For cloning of the soluble cytochrome c_{550}, pUC19-*cyc*A [57,58] was used as starting vector, carrying the *cyc*A-gene encoding the entire c_{550}.

pUC19-*cyc*A served as template for the following PCR using the primers cytc_{550}_NcoI: 5′-CTG CCC G**CC ATG G**CC CAG GAT GGC GAC GCC GCC AAA-3′ and cytc_{550}_HindIII: 5′-ATC TCG GAG GCG AAG CTT TCA

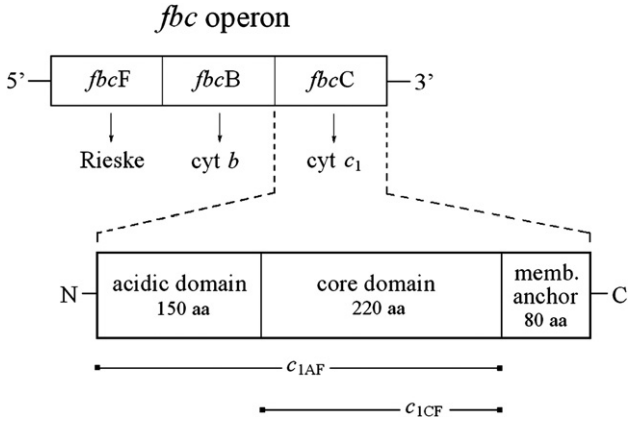

Fig. 1. Structure of the *fbc* operon from *Paracoccus denitrificans* [13], its translation products and the soluble c_{1CF} and c_{1AF} domains studied in this investigation (not drawn to scale).

GTT CGA TTC GCC CTC GGC-3′, which introduced a NcoI and HindIII site and yielded a 300 bp-product, which was cloned into pET-22b(+). Expression plasmids were transformed into *E. coli* BL21(DE3) (Novagen). Cotransformation with the heme maturation plasmid pEC86 [59] achieved efficient insertion of the heme cofactor into the apoproteins. Cells were grown at 37 °C in LB medium containing 100 μg/ml ampicillin and 60 μg/ml chloramphenicol.

Heterologous expression of c_{1CF} and c_{1AF} was induced by 0.4 mM isopropyl-1-thio-β-D-galactopyranoside (IPTG) at an OD_{600} of 1.2–1.4. After 4 h the reddish cells were harvested and the periplasmic fraction prepared [60], followed by purification of cytochromes at 4 °C via anion exchange chromatography using Q-Sepharose (Amersham Bioscience) in 50 mM Tris–HCl buffer pH 8, 1 mM EDTA, 50 mM NaCl (gradients: 50–500 mM NaCl for c_{1CF} and 350 mM–1 M for c_{1AF}) and gel filtration using Sephacryl S100 (Amersham Bioscience) in 50 mM Tris–HCl pH 8, 1 mM EDTA, 150 mM NaCl. Eluates and purification steps were analyzed by SDS-PAGE, heme staining and Western blot analysis (data not shown). The proteins displayed heme–protein ratios very close to 1 and the 695 nm charged-transfer band typical of *c*-type cytochromes with His–Met iron coordination, an indication that the heme moiety was properly inserted in the recombinant proteins.

Cytochrome c_{550} was expressed constitutively at 37 °C. Cells were harvested at an OD_{550} of around 3 and the protein was purified from the periplasm via anion exchange chromatography using Q-Sepharose (gradient: 50–350 mM NaCl) and gel filtration. The soluble cytochrome c_{552} fragment (c_{552F}) was expressed and purified as described by Reincke et al. [26].

Cytochrome concentrations were determined spectroscopically using the same extinction coefficient for all cytochromes $\Delta\varepsilon_{red\text{-}ox,\ \alpha\text{-}peak} = 19.4\ mM^{-1}\ cm^{-1}$ [22].

2.2. Difference spectra

Since cytochromes c_1 and c_{552} are spectroscopically very similar (Fig. 2) it was necessary to determine optimal wavelengths to follow the interprotein ET processes. Difference spectra using double sector cuvettes (DSC) were therefore recorded, the peaks and troughs of these spectra in the Soret and α-regions yielding detection wavelengths with minimal overlap and maximal resulting signal amplitude. The cytochromes were introduced in either sector of the DSC, with one cytochrome completely reduced (obtained by using N_2-flushed Tris buffer 20 mM pH 8 and pre-reduction of the cytochrome with dithionite, followed by Sephadex G25-chromatography to remove the excess reductant) and the other redox partner oxidized. A "before-mixing" (bm) and an "after-mixing" (am) spectrum were recorded (375–700 nm) and the difference spectrum generated by subtraction (am − bm). The DSC difference spectrum for the c_{1CF}/c_{552F} and c_{1CF}/c_{550} couples is shown in the inset to Fig. 2. In the Soret region the spectrum shows a peak and trough at 412 and 426.4 nm, respectively. These wavelengths were chosen to follow the ET reaction. Optimal wavelengths were determined for all the redox couples and yielded similar difference spectra.

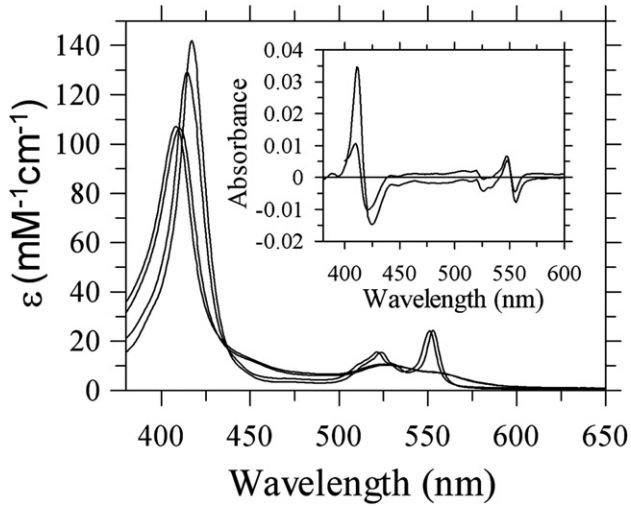

Fig. 2. Absorption spectra of c_{552F} and c_{1CF}. From left to right oxidized c_{552F} and c_{1CF} and reduced c_{552F} and c_{1CF}, respectively. The spectra have been generated from the extinction coefficients of 22.83 $mM^{-1}\ cm^{-1}$ (reduced-minus-oxidized at 553–537 nm) for c_{1CF} and of 21.16 $mM^{-1}\ cm^{-1}$ (reduced-minus-oxidized at 551-535 nm) for c_{552F}, both determined by the pyridine–hemochrome method. Inset. Double sector cuvette difference spectrum (after-minus-before mixing) of 3.05 μM ferro-c_{1CF} *vs.* 3.04 μM ferri-c_{552F} (top spectrum) or 1.50 μM ferro-c_{1CF} *vs.* 2.6 μM ferri-c_{550}. In both cases proteins were dissolved in 20 mM Tris–HCl pH 8, 1 mM EDTA. T=20 °C. 0.7 ml of protein solution was added to both chambers of the double sector cuvette. Light path: 0.8 cm. See Methods for details.

2.3. Stopped-flow spectroscopy

All kinetic experiments were carried out using a thermostatted Applied Photophysics stopped-flow apparatus (Leatherhead, UK) with a 1-cm observation chamber. Tris buffer (20 mM Tris–HCl pH 8, 1 mM EDTA) was used with the ionic strength adjusted by adding the appropriate amounts of KCl. All buffers and cytochrome solutions were flushed with nitrogen for 30 min to achieve anaerobic conditions to minimize autoxidation of the heme irons. Cytochrome c_1 fragments were pre-reduced with an excess of dithionite and passed over a Sephadex G25 column at 4 °C to remove the excess reductant. This is referred to as the dithionite protocol. Cytochrome c_{552F}, c_{550} and c_{551} from *Pseudomonas aeruginosa* ($c_{551\ Pa}$) were diluted in N_2-flushed Tris buffer. The pre-steady state kinetics at fixed ionic strength were performed at I=46 mM and 4.7 °C to slow down the ET reaction. All syringes were stored on ice before use and the solutions were equilibrated in the stopped-flow apparatus for 3 min before the measurements. Cytochrome c_{552F} (or c_{550} and $c_{551\ Pa}$) concentration was varied (1–10 μM) and measured against constant c_1 concentration (typically 3–5 μM; all concentrations are after mixing). The ET reaction was followed at a suitable wavelength as determined by DSC difference spectra (see above). Three to four kinetic traces were acquired for each individual condition, averaged and fitted to exponential functions to obtain the observed rate constants k_{obs} (see below). The apparent bimolecular rate constant was determined by linear regression of the observed rate constants as a function of the c_{552F} (or c_{550} and $c_{551\ Pa}$) concentrations.

Ionic strength measurements were performed with concentrations of cytochrome c_{1CF} comparable to its redox partners cytochrome c_{552F} and c_{550}. The cytochromes were diluted in Tris buffer (20 mM Tris–HCl pH 8, 1 mM EDTA; I=26 mM) and cytochrome c_{1CF} was pre-reduced as described above. The ionic strength was varied from 26 to 176 mM by addition of the appropriate amount of solid KCl. Measurements were carried out at 4.8 °C and followed at 412 nm and 410 nm. Four kinetic traces per salt condition were averaged. The ionic strength dependency of the observed rate constants was analysed according to the Brønsted law [61], shown in Eq. 1:

$$\log k = \log k_0 + 2 B z_A z_B \sqrt{I} \qquad (1)$$

where k is the observed rate constant at ionic strength I, k_0 is the rate constant at I=0, B is a term derived from Debye–Hückel equations with a value of ~0.5 at 5 °C and the product $z_A z_B$ the ET-sensitive effective interacting charges on the protein surfaces.

The above experiments were complicated by the spontaneous autoxidation of the cytochrome c_1 fragments (10% by the end of the experiments lasting 2–3 h), notwithstanding all solutions were carefully N_2-flushed. One set of experiments was therefore carried out according to the ascorbate protocol established for the *P. denitrificans* and *Thermus thermophilus* cytochrome c_{552}/Cu_A redox couple interaction [45]. In this protocol c_{1CF} is pre-reduced by ascorbate directly in the stopped-flow syringe and mixed with c_{552F}. To ensure that ascorbate would not interfer with the ET reaction of interest, the second-order rate constant for the reduction of c_{1CF} by ascorbate was determined. The experiment was carried out in Tris buffer at 4.8 °C and an ionic strength of I=46 mM. c_{1CF} concentration was kept constant (1.45 μM), with the ascorbate concentration being varied between 0.5 and 2.5 mM. The kinetics were monitored at 420 nm on a time scale of 200 s. Averaged time courses were fitted to an exponential function and yielded observed rate constants of 3.7×10^{-3} to $9.3\times10^{-3}\ s^{-1}$ as ascorbate concentration was increased from 0.5 to 2.5 mM. Linear regression of the pseudo-first order plot yielded an apparent bimolecular rate constant of 2.5 $M^{-1}\ s^{-1}$, which is 6 orders of magnitude slower than the ET reaction of interest (see Results). The ascorbate reduction of c_{1CF} and c_{1AF} turned out to be even slower than ascorbate reduction

of the soluble *Paracoccus* c_{552F} with an apparent bimolecular rate constant of 60 $M^{-1}s^{-1}$ [45]. Using this protocol the apparent second-order rate constant for the c_{1CF}/c_{552F} interaction was determined as a function of ionic strength in the range of 68–318 mM. Cytochrome c_{1CF} (3.8 μM) in N_2-flushed Tris buffer (10 mM Tris–HCl pH 8, 1 mM EDTA, 50 mM KCl) was pre-reduced with 1 mM ascorbate for at least 15 min in the stopped-flow syringe and mixed with c_{552F} whose concentration was varied (1–20 μM). Kinetics were performed at 10 °C and monitored at 424.6 nm.

2.4. Fitting procedures

In these experiments true pseudo-first order conditions could not be achieved and the concentrations of each redox couple was comparable (see above). There are three reasons for this choice. i) all the *c*-type cytochromes used in this study obviously share very similar spectra, yielding difference spectra with sharp peaks and troughs with low extinction changes (see Fig. 2); ii) the absolute absorbance in the Soret region was already very high under the present experimental conditions (typically 1–2 or higher absorbance units) and the α-band displayed extremely small changes; if true pseudo-first order conditions were to be used, we would have experienced saturation effects of the photomultiplier tube and deviations from Lambert–Beer's law; and iii) the observed ET processes are close to the time resolution of the stopped-flow apparatus (dead time ca. 1 ms). Data fitting was therefore performed by using equations for the analysis of bimolecular reactions under second-order conditions [62], Eq. 2:

$$A = A_0 + A_{EQ}\frac{1 - e^{-k_{OBS}t}}{1 + \omega\, e^{-k_{OBS}t}} \quad (2)$$

where A, A_0 and A_{EQ} are the observed absorbances at time t, $t = 0$, and at equilibrium, respectively, k_{OBS} the observed rate constant and ω a dimensionless parameter describing the deviation of the experimental conditions from pseudo-first order ($-1 < \omega < 1$, with $\omega = 0$ when true pseudo-first order conditions apply). The dependence of the observed rate constant of ferrous c_{1CF} oxidation on c_{552F} concentration was fitted to Eq. 3 [62]:

$$k_{OBS} = \sqrt{k_{FOR}^2(c_1 - c)^2 + 4k_{FOR}k_{REV}c_1 c} \quad (3)$$

where k_{FOR} and k_{REV} are the forward and reverse second order rate constants and c_1 and c the total c_{1CF} and c_{552F} concentrations, respectively. Data fitting was carried out by using the Origin 7.5 (OriginLab Corporation) software. The standard deviation of the fitted parameters never exceeded 10–15% unless otherwise stated.

3. Results

Soluble modules of redox protein complexes of the respiratory chain have been successfully used before to elucidate electron transport mechanisms [32,43–47,63]. In such experiments no detergents are required and only the ET reaction of interest is followed, avoiding kinetic interference by subsequent internal ET or energy transduction steps. The most likely mechanism for the interaction of these proteins is depicted in Scheme I:

$$c_1^{2+} + c^{3+} \underset{k_{REV}}{\overset{k_{FOR}}{\rightleftharpoons}} c_1^{3+} + c^{2+}$$

where c_1 represents either c_{1CF} and c_{1AF} and c the c_{552F} fragment or soluble cytochrome c_{550} from *Paracoccus denitrificans*, horse heart cytochrome *c* (c_{hh}) or cytochrome c_{551} from *Pseudomonas aeruginosa* (c_{551Pa}). k_{FOR} and k_{REV} are the second order rate constants. In this work we focus on the ET reaction of *P. denitrificans* cytochrome c_1 with its physiological and non-physiological redox partners to address the following issues: i) what general features characterize the ET between cytochrome c_1 and its substrates?, ii) is there a specificity or preference of c_1 for one of the two major physiological redox partners, cytochrome c_{552} or c_{550}?, iii) in what way does the unique N-terminal acidic domain of the *P. denitrificans* cytochrome c_1 influence the ET reactions?

3.1. Cloning, expression and purification of soluble ET fragments

Two different soluble fragments of the *P. denitrificans* cytochrome c_1 were cloned (Fig. 1): the 23.5 kDa c_1 core fragment (c_{1CF}), which only consists of the hydrophilic, redox-active heme-containing core domain and lacks the N-terminal acidic domain as well as the C-terminal membrane anchor. This core fragment represents the minimal functional redox unit of cytochrome c_1. The soluble 40.7 kDa cytochrome c_1 acidic fragment (c_{1AF}) lacks the C-terminal membrane anchor as well, but comprises in addition the unique, highly negatively charged, acidic domain of 150 amino acids.

As physiological redox partners of *P. denitrificans* cytochrome c_1, cytochrome c_{550} and a soluble fragment of cytochrome c_{552} (c_{552F}) were used. Cytochrome c_{550} is a small soluble cytochrome of 14 kDa and has been shown to play a major role in the respiratory pathways of denitrification [33,34], methanol oxidation and methylamine oxidation [35,36], but also to transfer electrons to the terminal cytochrome aa_3- and cbb_3-oxidases [37,58,64]. Cytochrome c_{552} is a membrane-bound cytochrome of 22 kDa. A cytochrome c_{552} mediated ET between the bc_1-complex and the aa_3 oxidase was confirmed by several studies on different supercomplexes containing the bc_1-complex, cytochrome c_{552}, aa_3-oxidase [23,24] and additionally complex I [25], as well as functional studies using antibodies against purified c_{552} and mutational studies working with c_{552} deletion strains [22]. Here a soluble, 100 amino acid fragment of cytochrome c_{552} (c_{552F}) was used [26].

All cytochromes were expressed heterologously in *E. coli* under aerobic conditions and yielded expression rates around 6 mg/L culture medium for both c_1-fragments (c_{1CF} and c_{1AF}) and up to 15 mg/L for cytochrome c_{550}. Purification was achieved by anion exchange chromatography and gel filtration. The purity of the cytochromes was determined by SDS-PAGE and immunologically characterized by Western blot analysis. Covalent heme incorporation was confirmed by heme staining, whereas redox activity and absorption properties were characterized spectroscopically (data not shown).

3.2. ET kinetics at constant ionic strength

Following redox reactions between two spectroscopically similar *c*-type cytochromes revealed the problem of spectral overlap (Fig. 2) and required the identification of suitable detection wavelengths. Recording difference spectra for each individual redox couple using double-sector cuvettes overcame this problem (see inset to Fig. 2 and Methods). Nevertheless, recording kinetic traces at these wavelengths meant to follow

ET on top of very high absorption levels due to high heme extinction in the Soret region (Fig. 2), so that the concentration range of the cytochrome being varied was restricted to low total heme concentrations for both redox proteins.

For a comparative study on the ET reactions of c_{1CF} and c_{1AF} with their redox partners, the ET reaction with cytochrome c_{552F} or c_{550} as physiological substrates was determined. Also, as non-physiological substrate used widely in turnover studies with the bc_1 complex, the highly positively charged horse heart cytochrome c_{hh}, and as a negative control, cytochrome c_{551Pa} from *Pseudomonas aeruginosa* [65] were used. Fig. 3 shows the time course of ET between c_{1CF} and c_{552F} as followed at 412 and 424.6 nm which correspond to peak and trough of the difference spectra, respectively (see inset to Fig. 2). The data could be fit to an exponential relaxation only poorly since in this experiment and in the following ones the concentrations of reagents were comparable in magnitude. Thus, the data were fit (solid lines in Fig. 3) to a second-order equation (Eq. (2)) which takes into account the prevalent non-pseudo first order conditions, i.e. stringent second-order conditions. The time course is complete within ca. 30–40 ms, thus the ET process is very fast with a loss of ca. 50% of the absorbance change, as determined from the fits (see solid lines in Fig. 3). Application of the Lambert–Beer law to the reaction mechanism in Scheme I implies that (Eq. 4):

$$\Delta A_{412\ \mathrm{nm}} = \frac{\left(\Delta\varepsilon^{412\ \mathrm{nm}}_{c_{552}} - \Delta\varepsilon^{412\ \mathrm{nm}}_{c_1}\right)}{\left(\Delta\varepsilon^{424.6\ \mathrm{nm}}_{c_{552}} - \Delta\varepsilon^{424.6\ \mathrm{nm}}_{c_1}\right)} \Delta A_{424.6\ \mathrm{nm}} \quad (4)$$

where the $\Delta\varepsilon$s are the reduced-minus-oxidized difference extinction coefficients at wavelengths 412 and 424.6 nm. The difference extinction coefficients were calculated from the data in Fig. 2: for c_1, $\Delta\varepsilon_{412\ nm} = -0.41\ mM^{-1}\ cm^{-1}$ and $\Delta\varepsilon_{424.6\ nm} = 46.47\ mM^{-1}\ cm^{-1}$; for c_{552F}, $\Delta\varepsilon_{412\ nm} = 27.40\ mM^{-1}\ cm^{-1}$ and $\Delta\varepsilon_{424.6\ nm} = 32.66\ mM^{-1}\ cm^{-1}$. Thus the expected dependence of the instantaneous absorption changes at one wavelength on the corresponding changes at a second wavelength is: $\Delta A_{412\ nm} = -2.01 \cdot \Delta A_{424.6\ nm}$. After plotting the absorbption changes at 412 nm *vs.* those at 424.6 nm (inset to Fig. 3) we obtain a slope of -1.80 ± 0.03 which is in good agreement with the expected slope of -2.01. These results strongly suggest a 1:1 stoichiometry of the reagents and products in Scheme I.

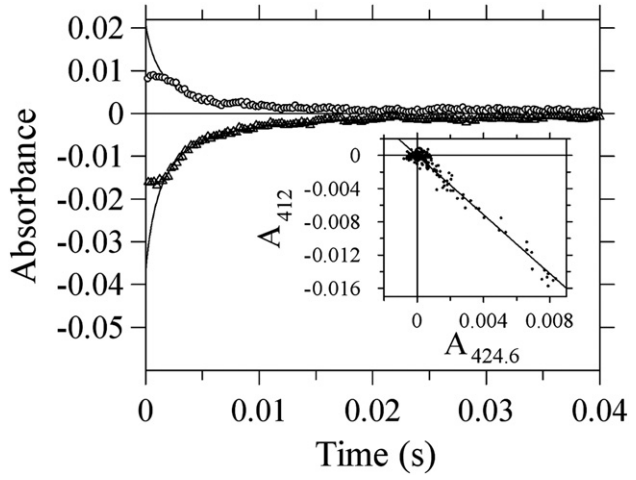

Fig. 3. Electron transfer between c_{1CF} (1.46 μM) and c_{552F} (1.18 μM) as followed at 412 (bottom trace) and 424.6 (top trace) nm. Concentrations are after mixing. Solid lines represent the fits according to Eq. (2). The fits were carried out simultaneously at the two wavelengths with the parameters k_{OBS} and ω being shared: $k_{OBS} = 113.0 \pm 7.1\ s^{-1}$, $\omega = -0.86 \pm 0.02$. At 412 nm the fitted amplitudes are: $A_0 = -0.037 \pm 0.002$, $A_{EQ} = 0.036 \pm 0.002$; at 424.6 nm the fitted amplitudes are: $A_0 = 0.021 \pm 0.001$ $A_{EQ} = -0.021 \pm 0.001$. The first 5 time points (ca. 2 ms) of the total of 400 were excluded from the fits since this represents the flow period of the stopped-flow apparatus. $T = 4.7$ °C, $I = 46$ mM. Inset: plot of the absorbance at 412 nm *vs.* the absorbance at 424.6 nm. Solid line is the linear regression of the data points with a slope of -1.80 ± 0.03 and a *Y*-intercept of $0 \pm 7\ 10^{-5}$.

Table 1
Bimolecular rate constants and relative specificity derived from pre-steady state kinetics at fixed ionic strength (46 mM) for the ET reactions of c_{1CF} and c_{1AF} with c_{552F}, c_{550}, c_{hh} and c_{551Pa}

Redox couple	k ($M^{-1}s^{-1}$)[a]	k (c_{1CF})/k(c_{1AF})
c_{1CF}/c_{552F}	3.4×10^7	1
c_{1AF}/c_{552F}	3.3×10^7	0.97
c_{1CF}/c_{550}	9.1×10^7	1
c_{1AF}/c_{550}	9.3×10^7	1.02
c_{1CF}/c_{hh}	1.3×10^8	1
c_{1AF}/c_{hh}	9.7×10^7	0.75
$c_{1CF}/c_{551\ Pa}$	3.5×10^3	1
$c_{1AF}/c_{551\ Pa}$	1.9×10^4	5.43

[a] All fitting errors in the second-order rate constants are within 10–15%.

In general the ET reaction of c_{1CF} and c_{1AF} with their substrates turned out to be very fast (apparent bimolecular rate constants of 10^7 to $10^8\ M^{-1}s^{-1}$), approaching the limit imposed by diffusion (see Table 1). The mechanism of ET between two partners must involve a binding reaction, the actual ET process in which an electron is exchanged within the collisional complex, and the dissociation of products. In the present experiments what we measure is the overall ET rate with a very fast ET event within the collisional complex.

For a direct comparison of the ET of c_{1CF} and c_{1AF} with the same substrate, the measured apparent bimolecular rate constant k of c_{1AF} is normalized to the corresponding rate constant of c_{1CF} (Table 1). The reaction of cytochrome c_{1CF} and c_{1AF} with their physiological redox partner cytochrome c_{552F} yielded apparent bimolecular rate constants of $3.4 \times 10^7\ M^{-1}s^{-1}$ and $3.3 \times 10^7\ M^{-1}s^{-1}$ for c_{1CF} and c_{1AF}, respectively, indicating no preference of the acidic fragment over the core fragment. The ET reaction of c_{1CF} or c_{1AF} with cytochrome c_{550} revealed similar rates and displayed likewise no preference for c_{1AF} over c_{1CF} at all. This finding indicates no direct contribution of the acidic domain to the interactions with the physiological redox partners cytochromes c_{552} and c_{550}.

To assess the specificity of the ET interactions, the c_1 fragments were also probed, under identical conditions, with two non-physiological cytochromes *c* proteins: horse heart cytochrome *c* (c_{hh}), a highly positively charged soluble cytochrome, and *Pseudomonas aeruginosa* cytochrome c_{551} (c_{551Pa}). In the case of c_{hh} the ET with both cytochrome c_1-fragments was accelerated 3- to 4-fold when compared to c_{552F} (1.3×10^8 and $9.7 \times 10^7\ M^{-1}s^{-1}$ for c_{1CF} and c_{1AF}, respectively, see Table 1). This is likely to be due to the higher positive surface charge of c_{hh} which enhances the driving force of the reaction.

Similar to the situation in the yeast cytochrome c_1 [50] modeling approaches for the *Paracoccus* c_1 core fragment (data not shown) display surface exposed patches of negatively charged residues in the peripheral surrounding of the heme crevice. This indicates a strong electrostatic component in the ET reaction. Although c_{550} has just a slightly higher p*I* than c_{552F} (4.85 and 4.59, respectively), it reacted more than twice as fast with c_{1CF}/c_{1AF}, suggesting that also non-polar forces contribute to the interaction and have a strong influence on forming a proper ET complex.

The reaction of c_{hh} with c_{1AF} is decreased by approximately 25% compared to c_{1CF} (Table 1). This effect was unexpected assuming the high surface charge of both proteins would drive the interaction and confirms the proposal discussed above that the acidic domain does not contribute directly to the ET interactions. We speculate that the acidic domain may sequester some fraction of the c_{hh} by locking it into a tight electrostatic complex unavailable for efficient ET, reducing the effective c_{hh} concentration and therefore the apparent bimolecular rate constant.

Cytochrome c_{551} from *Pseudomonas aeruginosa* is a small, soluble cytochrome. Its heme crevice is dominated by hydrophobic side chains, conferring a rather apolar character [65]. When mixed in the stopped-flow apparatus with both c_1 fragments under otherwise identical conditions, the experiments yielded apparent bimolecular rates of $3.5 \cdot 10^3$ $M^{-1}s^{-1}$ for c_{1CF} and $1.9 \cdot 10^4$ $M^{-1}s^{-1}$ for c_{1AF} (Table 1), which are between 3–4 orders of magnitude slower than the ET reaction between the physiological redox partners. This effect can be explained by

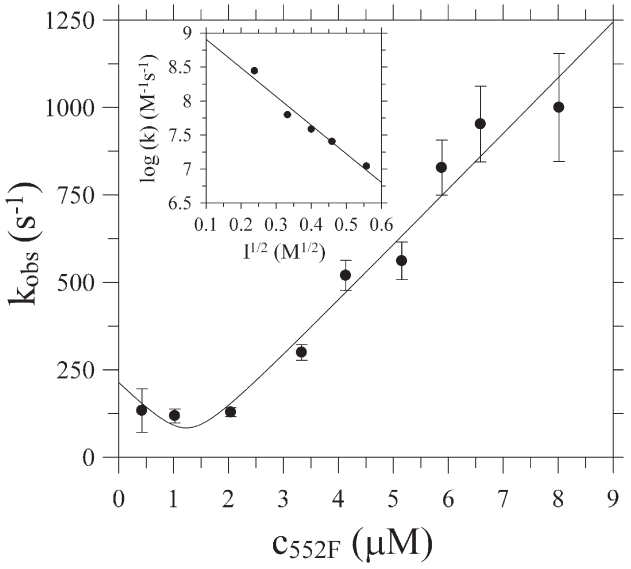

Fig. 4. ET reaction of c_{1CF} with c_{552F} in the presence of ascorbate. 1.9 μM c_{1CF} pre-reduced with 0.5 mM ascorbate was mixed in the stopped-flow apparatus with 0.5–10 μM c_{552F} and the time courses followed at 412 or 424.6 nm at an ionic strength of 61 mM and T=9.8 °C. All concentrations are after mixing.The averaged time courses were fitted to Eq. (2) and the determined rate constants plotted as a function of c_{552F} concentration. The solid line is the best fit to Eq. (3). The slope of the linear portion of the plot yields the apparent second-order rate constant k_{FOR} and the non-linearity at low c_{552F} concentrations is due to the deviation from pseudo-first order conditions. The fitted value of k_{REV} displayed a very large fitting error and is not given here. Inset: Ionic strength dependence of the apparent second-order rate constants.

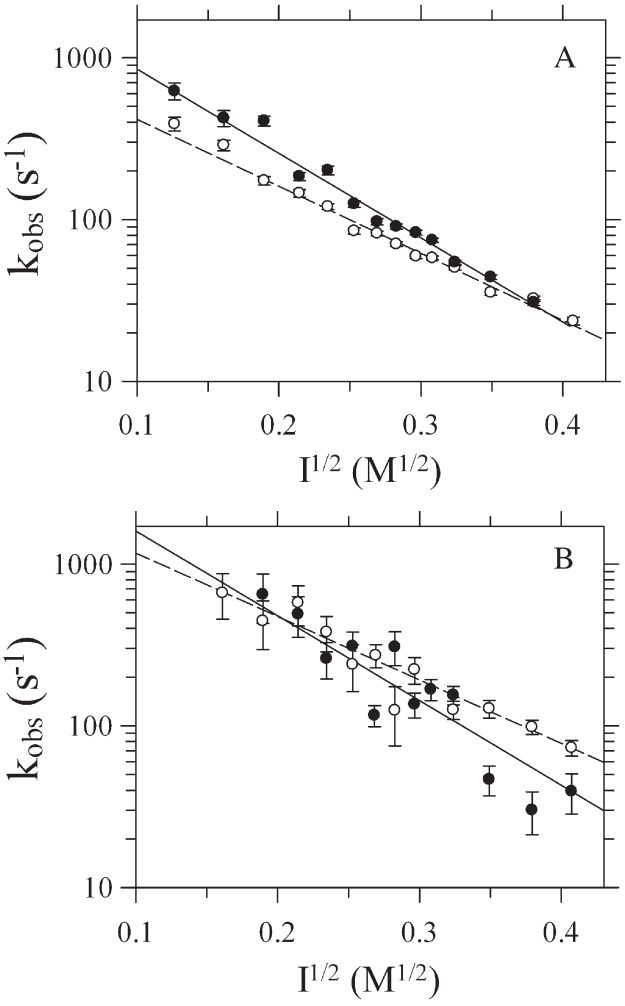

Fig. 5. Ionic strength dependency for the ET reaction of cytochrome c_{1CF} (filled circles) and c_{1AF} (open circles) with *P. d.* c_{552F} (A) and c_{550} (B). According to the Brønsted law the logarithm of the observed rate constants is plotted as a function of the square root of ionic strength, the product $z_A z_B$ is derived from the slope and reflects the product of effective interacting charges on each protein surface. The concentrations were c_{1CF} (3.04 μM) *vs.* c_{552F} (6.02 μM), c_{1AF} (3.04 μM) *vs.* c_{552F} (5.23 μM) c_{1AF} (3.01 μM) *vs.* c_{550} (5.29 μM) c_{1CF} (2.86 μM) *vs.* c_{550} (4.05 μM). All ET reactions were followed at 412 nm at 4.7 °C. Solid and dashed lines are best fits to Eq. (1).

the hydrophobic character of the c_{551Pa} heme hemisphere and the lack of the highly positive charge cluster around its heme cleft required to electrostatically direct the association of both redox partners. Taken together the kinetic results of the ET reaction of c_{1CF} and c_{1AF} with their different redox partners (c_{552F}, c_{hh} and c_{551Pa}) demonstrate that i) the charge distribution around the heme cleft plays a major role in association of both redox partners due to the overall electrostatic dipole momentum. ii) the p*I*-value of the proteins as a general surface charge parameter does not reflect the relative specificity, and iii) direct hydrophobic contacts and the interface properties may be important for a proper ET complex formation.

In the above experiments the c_1 fragments were initially reduced with dithionite and the excess reductant removed by gel filtration. This procedure allowed to mix the fully reduced proteins with various electron acceptors. Nevertheless,

cytochrome c_1 fragments autoxidized spontaneously over several hours of time. Although in each experiment the concentrations of ferrocytochrome c_1 fragments were determined at the end of the experiments (autoxidation never exceeded 10%) it was of interest to study the same reactions in the presence of a slow reductant such as ascorbate. Following a previously used experimental protocol [45,46] cytochrome c_1 fragments were reduced with 1 mM ascorbate directly in the stopped-flow syringe and ET followed as described above (ascorbate protocol, see Methods). The results of a typical experiment, carried out at an ionic strength of 61 mM are shown in Fig. 4 for the c_{1CF}/c_{552F} couple. At this ionic strength the measured apparent bimolecular rate constant is $2.8 \cdot 10^8$ $M^{-1}s^{-1}$ and decreased to $1.1 \cdot 10^7$ $M^{-1}s^{-1}$ at I=311 mM. The inset to Fig. 4 shows that the second-order rate contants display an ionic strength dependence very similar to that obtained when using the experimental protocol in the absence of exogenous reductants with an extrapolated rate constant of 2.1×10^9 $M^{-1}s^{-1}$ at zero ionic strength and a $z_A z_B$ product of ca. 2.1.

3.3. Ionic strength dependencies

To further investigate the electrostatic character of the ET reaction and to clarify the issue of the contribution of the acidic domain to ET-complex formation, the ionic strength dependency of the ET rates for the c_{1CF} and c_{1AF} reactions with their physiological redox partners c_{552F} and c_{550} were probed and analyzed according to Eq. (1) (see Methods). Each ET couple yielded rates decreasing linearly with increasing ionic strength when plotted according to Eq. (1). The resulting slopes ($z_A z_B$ product in Eq. (1)) are negative, indicating interacting charges of opposite sign on either protein. The results are presented in Fig. 5 and the Brønsted parameters listed in Table 2. According to this analysis there are 2.3 (c_{1CF}/c_{552F} couple) and 2.1 (c_{1AF}/c_{552F} couple) effective charges on each protein surface and a somewhat higher charge contribution of the core fragment compared to the acidic (Fig. 5A). The reaction of c_{1CF} and c_{1AF} with c_{550} displayed similar Brønsted slopes (Fig. 5B) with 2.5 (c_{1CF}) and 2.3 (c_{1AF}) effective charges and a slightly higher charge contribution of c_{1CF} over c_{1AF} as well. Taken together, 2–3 charges are involved in ET interactions of the cytochrome c_1 fragments with c_{552F} and c_{550}, clearly indicating Coulombic forces in association. These values are in good agreement with the number of 2–3 effective charges interacting for the *P. denitrificans* c_{552F}/Cu_A redox couple [45,46] supporting the idea that native c_{552} mediates the ET reaction between cytochrome c_1 and aa_3-oxidase in an oriented way using the same interaction interface for both redox partners.

Table 2
Brønsted parameters of the ionic strength dependency measurements of c_{1CF}/c_{1AF} with c_{552F}/c_{550} in comparison

Redox couple	$z_A z_B$	Effective charges
c_{1CF}/c_{552F}	−5.21±0.10	2.3
c_{1AF}/c_{552F}	−4.14±0.08	2.0
c_{1CF}/c_{550}	−5.24±0.61	2.3
c_{1AF}/c_{550}	−3.92±0.37	2.0

The rates for the ET reaction of c_{1CF}/c_{1AF} with c_{550} compared to the c_{552} were increased, pointing at a more efficient ET with c_{550} and confirming the different functional role of c_{550} in the branched respiratory chain of *P. denitrificans*. No evidence could be found for any direct involvement of the acidic domain to the ET process.

Finally, engineering of the c_1 soluble domains exposes an additional heme edge to the solvent corresponding to the surface which interacts with the Rieske protein in holo-bc_1. This site, referred to as the R-side (as opposed to the C-side), is a potential site for ET to or from c_{552F} and c_{550}. We have carried out a structural modeling of the *P. denitrificans* cytochrome c_1 sequence onto the yeast c_1 structure (pdb: 1KYO). From this analysis (not shown) it appears that on the R-side the heme edge is enclosed within an anular cluster of basic residues, whereas the C-side displays a less evident cluster of acidic residues. The C-side carries, therefore, the proper structural determinants to interact favourably with the extensively basic c_{552F} [27] (pdb: 1QL4) and c_{550} surfaces and leaving the R-side as an unlikely though not excluded target candidate.

4. Discussion

When the apparent bimolecular rate constants of both c_1-fragments with each electron acceptor (c_{552}, c_{550}, c_{hh} and c_{551Pa}) are compared, it follows that the ET reaction of c_{1CF} or c_{1AF} with c_{550} is approximately 3 times faster than the reaction with c_{552F} (Table 1). Thus c_{550} is a more efficient electron acceptor than c_{552F}, suggesting different roles for these cytochromes in the respiratory chain of *P. denitrificans*. As has been determined previously [22–25,37], cytochrome c_{552} is the genuine electron mediator between the bc_1-complex and aa_3-oxidase, a respiratory branch operative under high oxygen concentrations. Although cytochrome c_{550} is predominantly expressed under anaerobic conditions with nitrate as the terminal electron acceptor [57,58], it is also present under aerobic conditions to some extent and able to accept electrons. Under microaerophilic and thus potentially denitrifying conditions, however, when the expression of the cbb_3-oxidase and the nitrite reductase is induced, cytochrome c_{550} is the essential electron mediator and readily available to transfer electrons. The more efficient reaction between cytochrome c_1 and c_{550} supports efficient ET, eventually allowing energy transduction even under energetically unfavourable conditions by switching the ET in the redox chain immediately to the denitrifying branch. In the native cytochrome c_{552} the heme domain is not only recruited to the membrane by its membrane anchor, but the protein has also been shown to be a component of a supercomplex of defined stoichiometry comprising the bc_1-complex, aa_3-oxidase and complex I [23,25], thus allowing efficient ET.

At variance with this situation, under a shift from microaerophilic to anaerobic conditions, ET reactions suffer from the fact the final electron acceptor oxygen is scarce or almost absent, making the aa_3-type oxidase with its very low affinity for oxygen [69] a poor player in energy transduction processes,

while on the other hand the cbb_3 terminal oxidase optimized for such low O_2 conditions [70] lacks an efficient supply of electrons. If this cbb_3 oxidase (and, e.g. also the nitrite reductase) is ET-linked to the soluble c_{550} only by a diffusion-based mechanism, the preponderance of a supercomplex-based ET efficiency (via the cytochrome c_{552}) needs to be overcome by a more efficient ET reaction from cytochrome c_{550} to its interaction partners to efficiently maintain ET-coupled energy transduction under such conditions.

All kinetic experiments involving the two soluble cytochrome c_1-fragments and their homologous redox partners reveal high ET rates, approaching the limit of a diffusion-controlled reaction. This indicates transient and short-lived ET complexes but specific and therefore very fast and efficient ET. A strong positive Coulomb effect on complex association is exerted both by the two physiological redox partners, cytochrome c_{550} and c_{552} of *P. denitrificans*, as well as by the highly positively charged horse heart cytochrome *c* (positive control), but is absent in the reaction with the *P. aeruginosa* cytochrome c_{551} providing an apolar docking site (used as a negative control). Even though displaying a slight negative overall charge, both *Paracoccus* cytochromes, along with the non-physiological horse heart cytochrome c_{hh}, share a highly positive surface charge around their heme crevices. The electrostatic nature of the interaction is further quantified by ionic strength dependency measurements, showing a number of 2–3 effective charges of opposite sign present on each of the two interacting protein surfaces. The unique acidic domain of the *Paracoccus* cytochrome c_1 does not directly contribute to ET interactions, for no drastic difference in the ionic strength behaviour of the c_{1AF} relative to c_{1CF} is observed. This may suggest a function of the acidic domain other than guiding the positively charged heme crevices of cytochromes c_{552} or c_{550} via long-range electrostatics as some kind of "docking platform" to the correct reaction interface of cytochrome c_1, in contrast to the "hinge" function of subunit 6 in yeast or subunit 8 in bovine bc_1-complex [15,16,19,50]. The fast bimolecular rates (ca. 10^8 $M^{-1}s^{-1}$) for the ET reactions of cytochrome c_1 with its redox partners together with the ionic strength dependencies and the number of 2–3 effective charges derived from Brønsted analysis confirm previous observations regarding *Paracoccus* native cytochrome c_{552} and aa_3-oxidase [32] and fit very well to the results of Maneg et al. [45] for the *P. denitrificans* Cu_A/c_{552F} redox couple, underlining the existing complex-formation model for transient ET complexes [32,44,45,66,67]. The results of this investigation are also consistent with the findings of [68] in which a photooxidized ruthenium-cytochrome *c* derivative was used to study the electron transfer kinetics with yeast cytochrome c_1 within the entire complex III. Comparing rate constants of cytochrome c_{1CF}/c_{1AF} with both their physiological redox partners c_{552} and c_{550}, a preference of cytochrome c_{550} over cytochrome c_{552} is observed which underlines the different functions of both cytochromes within the respiratory chain of *P. denitrificans*. It should be kept in mind, though, that this study has been performed with soluble fragments, providing a higher degree of diffusional freedom for the proteins to interact in solution, compared to the c_1 domain being membrane-anchored, integrated in a bc_1 complex and organized in a supercomplex assembly, where much higher physical constraints are exerted in terms of directionality of ET interactions.

Acknowledgements

We thank Hans-Werner Müller for excellent technical assistance and acknowledge the financial support by Deutsche Forschungsgemeinschaft (SFB 472). We also thank Maurizio Brunori (Sapienza University of Rome, Italy) for making the stopped-flow apparatus available to us, and Francesca Cutruzzolà (Sapienza University of Rome, Italy) for providing us a sample of *Pseudomonas aeruginosa* cytochrome c_{551}.

References

[1] Z.L. Zhang, L.S. Huang, V.M. Shulmeister, Y.I. Chi, K.K. Kim, L.W. Hung, A.R. Crofts, E.A. Berry, S.H. Kim, Electron transfer by domain movement in cytochrome bc_1, Nature 392 (1998) 677–684.
[2] C. Breyton, The cytochrome b(6)f complex: structural studies and comparison with the bc(1) complex, Biochim. Biophys. Acta 1459 (2000) 467–474.
[3] P. Mitchell, The protonmotive Q cycle: a general formulation, FEBS Lett. 59 (1975) 137–139.
[4] P. Mitchell, Possible molecular mechanisms of the protonmotive function of cytochrome systems, J. Theor. Biol. 62 (1976) 327–367.
[5] E.B. Gutierrez-Cirlos, B.L. Trumpower, Inhibitory analogs of ubiquinol act anti-cooperatively on the Yeast cytochrome bc_1 complex. Evidence for an alternating, half-of-the-sites mechanism of ubiquinol oxidation, J. Biol. Chem. 277 (2002) 1195–1202.
[6] Y. Zu, M.M. Couture, D.R. Kolling, A.R. Crofts, L.D. Eltis, J.A. Fee, J. Hirst, Reduction potentials of Rieske clusters: importance of the coupling between oxidation state and histidine protonation state, Biochemistry 42 (2003) 12400–12408.
[7] A. Osyczka, C.C. Moser, P.L. Dutton, Fixing the Q cycle, Trends Biochem. Sci. 30 (2005) 176–182.
[8] C.A. Yu, J.Z. Xia, A.M. Kachurin, L. Yu, D. Xia, H. Kim, J. Deisenhofer, Crystallization and preliminary structure of beef heart mitochondrial cytochrome-bc_1 complex, Biochim. Biophys. Acta 1275 (1996) 47–53.
[9] D. Xia, C.A. Yu, H. Kim, J.Z. Xia, A.M. Kachurin, L. Zhang, L. Yu, J. Deisenhofer, Crystal structure of the cytochrome bc_1 complex from bovine heart mitochondria, Science 277 (1997) 60–66.
[10] S. Iwata, J.W. Lee, K. Okada, J.K. Lee, M. Iwata, B. Rasmussen, T.A. Link, S. Ramaswamy, B.K. Jap, Complete structure of the 11-subunit bovine mitochondrial cytochrome bc_1 complex, Science 281 (1998) 64–71.
[11] C. Hunte, J. Koepke, C. Lange, T. Rossmanith, H. Michel, Structure at 2.3 Å resolution of the cytochrome bc(1) complex from the yeast *Saccharomyces cerevisiae* co-crystallized with an antibody Fv fragment, Structure 8 (2000) 669–684.
[12] C. Hunte, S. Solmaz, C. Lange, Electron transfer between yeast cytochrome bc(1) complex and cytochrome *c*: a structural analysis, Biochim. Biophys. Acta 1555 (2002) 21–28.
[13] B. Kurowski, B. Ludwig, The genes of the *Paracoccus denitrificans* bc_1 complex. Nucleotide sequence and homologies between bacterial and mitochondrial subunits, J. Biol. Chem. 262 (1987) 13805–13811.
[14] B. Ludwig, K. Suda, N. Cerletti, Cytochrome c_1 from *Paracoccus denitrificans*, Eur. J. Biochem. 137 (1983) 597–602.
[15] C.H. Kim, T.E. King, A mitochondrial protein essential for the formation of the cytochrome *c*1-*c* complex. Isolation, purification, and properties, J. Biol. Chem. 258 (1983) 13543–13551.
[16] C.H. Kim, C. Balny, T.E. King, Role of the hinge protein in the electron transfer between cardiac cytochrome c_1 and *c*. Equilibrium constants and kinetic probes, J. Biol. Chem. 262 (1987) 8103–8108.
[17] S. Ohta, K. Goto, H. Arai, Y. Kagawa, An extremely acidic amino-terminal presequence of the precursor for the human mitochondrial hinge protein, FEBS Lett. 226 (1987) 171–175.

[18] C.H. Kim, R.S. Zitomer, Disruption of the gene encoding subunit VI of yeast cytochrome bc_1 complex causes respiratory deficiency of cells with reduced cytochrome *c* levels, FEBS Lett. 266 (1990) 78–82.
[19] J. Stonehuerner, P. O'Brien, L. Geren, F. Millett, J. Steidl, L. Yu, C.A. Yu, Identification of the binding site on cytochrome c_1 for cytochrome *c*, J. Biol. Chem. 260 (1985) 5392–5398.
[20] M.E. Schmitt, B.L. Trumpower, Subunit 6 regulates half-of-the-sites reactivity of the dimeric cytochrome bc_1 complex in *Saccharomyces cerevisiae*, J. Biol. Chem. 265 (1990) 17005–17011.
[21] M. Nakai, T. Endo, T. Hase, Y. Tanaka, B.L. Trumpower, H. Ishiwatari, A. Asada, M. Bogaki, H. Matsubara, Acidic regions of cytochrome c_1 are essential for ubiquinol-cytochrome *c* reductase activity in yeast cells lacking the acidic QCR6 protein, J. Biochem. (Tokyo) 114 (1993) 919–925.
[22] A. Turba, M. Jetzek, B. Ludwig, Purification of *Paracoccus denitrificans* cytochrome c_{552} and sequence analysis of the gene, Eur. J. Biochem. 231 (1995) 259–265.
[23] E.A. Berry, B.L. Trumpower, Isolation of ubiquinol oxidase from *Paracoccus denitrificans* and resolution into cytochrome bc_1 and cytochrome *c*-aa_3 complexes, J. Biol. Chem. 260 (1985) 2458–2467.
[24] T. Haltia, A. Puustinen, M. Finel, The *Paracoccus denitrificans* cytochrome aa_3 has a third subunit, Eur. J. Biochem. 172 (1988) 543–546.
[25] A. Stroh, O. Anderka, K. Pfeiffer, T. Yagi, M. Finel, B. Ludwig, H. Schagger, Assembly of respiratory complexes I, III, and IV into NADH oxidase supercomplex stabilizes complex I in *Paracoccus denitrificans*, J. Biol. Chem. 279 (2004) 5000–5007.
[26] B. Reincke, L. Thöny-Meyer, C. Dannehl, A. Odenwald, M. Aidim, H. Witt, H. Rüterjans, B. Ludwig, Heterologous expression of soluble fragments of cytochrome c_{552} acting as electron donor to the *Paracoccus denitrificans* cytochrome *c* oxidase, Biochim. Biophys. Acta 1411 (1999) 114–120.
[27] A. Harrenga, B. Reincke, H. Rüterjans, B. Ludwig, H. Michel, Structure of the soluble domain of cytochrome *c*(552) from *Paracoccus denitrificans* in the oxidized and reduced states, J. Mol. Biol. 295 (2000) 667–678.
[28] C. Lücke, B. Reincke, F. Lohr, P. Pristovsek, B. Ludwig, H. Rüterjans, Complete ^{1}H, ^{15}N and ^{13}C assignment of the functional domain of *Paracoccus denitrificans* cytochrome c_{552} in the oxidized state, J. Biomol. NMR 18 (2000) 365–366.
[29] P. Pristovsek, C. Lücke, B. Reincke, F. Löhr, B. Ludwig, H. Rüterjans, Complete ^{1}H, ^{15}N and ^{13}C assignment of the functional domain of *Paracoccus denitrificans* cytochrome c_{552} in the reduced state, J. Biomol. NMR 16 (2000) 353–354.
[30] P. Pristovsek, C. Lücke, B. Reincke, B. Ludwig, H. Rüterjans, Solution structure of the functional domain of *Paracoccus denitrificans* cytochrome c_{552} in the reduced state, Eur. J. Biochem. 267 (2000) 4205–4212.
[31] H. Wienk, O. Maneg, C. Lücke, P. Pristovsek, F. Löhr, B. Ludwig, H. Rüterjans, Interaction of cytochrome *c* with cytochrome *c* oxidase: an NMR study on two soluble fragments derived from *Paracoccus denitrificans*, Biochemistry 42 (2003) 6005–6012.
[32] V. Drosou, B. Reincke, M. Schneider, B. Ludwig, Specificity of the interaction between the *Paracoccus denitrificans* oxidase and its substrate cytochrome *c*: comparing the mitochondrial to the homologous bacterial cytochrome *c*(552), and its truncated and site-directed mutants, Biochemistry 41 (2002) 10629–10634.
[33] F.C. Boogerd, H.W. van Verseveld, A.H. Stouthamer, Electron transport to nitrous oxide in *Paracoccus denitrificans*, FEBS Lett. 113 (1980) 279–284.
[34] I. Matchova, I. Kucera, Evidence for the role of soluble cytochrome *c* in the dissimilatory reduction of nitrite and nitrous oxide by cells of *Paracoccus denitrificans*, Biochim. Biophys. Acta 1058 (1991) 256–260.
[35] J.W. de Gier, M. Lubben, W.N. Reijnders, C.A. Tipker, D.J. Slotboom, R.J. van Spanning, A.H. Stouthamer, J. van der Oost, The terminal oxidases of *Paracoccus denitrificans*, Mol. Microbiol. 13 (1994) 183–196.
[36] V.L. Davidson, M.A. Kumar, Cytochrome *c*-550 mediates electron transfer from inducible periplasmic *c*-type cytochromes to the cytoplasmic membrane of *Paracoccus denitrificans*, FEBS Lett. 245 (1989) 271–273.
[37] M.F. Otten, J. van der Oost, W.N. Reijnders, H.V. Westerhoff, B. Ludwig, R.J. Van Spanning, Cytochromes *c*(550), *c*(552), and *c*(1) in the electron transport network of *Paracoccus denitrificans*: redundant or subtly different in function? J. Bacteriol. 183 (2001) 7017–7026.
[38] W.H. Koppenol, E. Margoliash, The asymmetric distribution of charges on the surface of horse cytochrome *c*. Functional implications, J. Biol. Chem. 257 (1982) 4426–4437.
[39] S.H. Speck, S. Ferguson-Miller, N. Osheroff, E. Margoliash, Definition of cytochrome *c* binding domains by chemical modification: kinetics of reaction with beef mitochondrial reductase and functional organization of the respiratory chain, Proc. Natl. Acad. Sci. U. S. A. 76 (1979) 155–159.
[40] R. Rieder, H.R. Bosshard, Comparison of the binding sites on cytochrome *c* for cytochrome *c* oxidase, cytochrome bc_1, and cytochrome c_1. Differential acetylation of lysyl residues in free and complexed cytochrome *c*, J. Biol. Chem. 255 (1980) 4732–4739.
[41] J. Hall, X.H. Zha, B. Durham, P. O'Brien, B. Vieira, D. Davis, M. Okamura, F. Millett, Reaction of cytochromes *c* and c_2 with the *Rhodobacter sphaeroides* reaction center involves the heme crevice domain, Biochemistry 26 (1987) 4494–4500.
[42] J. Hall, X.H. Zha, L. Yu, C.A. Yu, F. Millett, Role of specific lysine residues in the reaction of *Rhodobacter sphaeroides* cytochrome c_2 with the cytochrome bc_1 complex, Biochemistry 28 (1989) 2568–2571.
[43] P. Lappalainen, N.J. Watmough, C. Greenwood, M. Saraste, Electron transfer between cytochrome *c* and the isolated Cu_A domain: identification of substrate-binding residues in cytochrome *c* oxidase, Biochemistry 34 (1995) 5824–5830.
[44] V. Drosou, F. Malatesta, B. Ludwig, Mutations in the docking site for cytochrome *c* on the *Paracoccus* heme aa_3 oxidase. Electron entry and kinetic phases of the reaction, Eur. J. Biochem. 269 (2002) 2980–2988.
[45] O. Maneg, B. Ludwig, F. Malatesta, Different interaction modes of two cytochrome-*c* oxidase soluble Cu_A fragments with their substrates, J. Biol. Chem. 278 (2003) 46734–46740.
[46] O. Maneg, F. Malatesta, B. Ludwig, V. Drosou, Interaction of cytochrome *c* with cytochrome oxidase: two different docking scenarios, Biochim. Biophys. Acta 1655 (2004) 274–281.
[47] D. Mooser, O. Maneg, C. Corvey, T. Steiner, F. Malatesta, M. Karas, T. Soulimane, B. Ludwig, A four-subunit cytochrome *bc*(1) complex complements the respiratory chain of *Thermus thermophilus*, Biochim. Biophys. Acta 1708 (2005) 262–274.
[48] H. Pelletier, J. Kraut, Crystal structure of a complex between electron transfer partners, cytochrome *c* peroxidase and cytochrome *c*, Science 258 (1992) 1748–1755.
[49] H.L. Axelrod, E.C. Abresch, M.Y. Okamura, A.P. Yeh, D.C. Rees, G. Feher, X-ray structure determination of the cytochrome c_2: reaction center electron transfer complex from *Rhodobacter sphaeroides*, J. Mol. Biol. 319 (2002) 501–515.
[50] C. Lange, C. Hunte, Crystal structure of the yeast cytochrome bc_1 complex with its bound substrate cytochrome *c*, Proc. Natl. Acad. Sci. U. S. A. 99 (2002) 2800–2805.
[51] L. Chen, R.C. Durley, F.S. Mathews, V.L. Davidson, Structure of an electron transfer complex: methylamine dehydrogenase, amicyanin, and cytochrome c_{551i}, Science 264 (1994) 86–90.
[52] V.L. Davidson, L.H. Jones, Electron transfer from copper to heme within the methylamine dehydrogenase-amicyanin-cytochrome c_{551i} complex, Biochemistry 35 (1996) 8120–8125.
[53] H.B. Brooks, V.L. Davidson, Kinetic and thermodynamic analysis of a physiologic intermolecular electron-transfer reaction between methylamine dehydrogenase and amicyanin, Biochemistry 33 (1994) 5696–5701.
[54] J.A. Worrall, U. Kolczak, G.W. Canters, M. Ubbink, Interaction of yeast iso-1-cytochrome *c* with cytochrome *c* peroxidase investigated by [^{15}N, ^{1}H] heteronuclear NMR spectroscopy, Biochemistry 40 (2001) 7069–7076.
[55] C.C. Moser, P.L. Dutton, Cytochrome *c* and c_2 binding dynamics and electron transfer with photosynthetic reaction center protein and other integral membrane redox proteins, Biochemistry 27 (1988) 2450–2461.
[56] P.B. Crowley, M.A. Carrondo, The architecture of the binding site in redox protein complexes: implications for fast dissociation, Proteins 55 (2004) 603–612.

[57] P.B. Scholes, G. McLain, L. Smith, Purification and properties of a *c*-type cytochrome from *Micrococcus denitrificans*, Biochemistry 10 (1971) 2072–2076.
[58] S.C. Baker, S.J. Ferguson, B. Ludwig, M.D. Page, O.M. Richter, R.J. van Spanning, Molecular genetics of the genus *Paracoccus*: metabolically versatile bacteria with bioenergetic flexibility, Microbiol. Mol. Biol. Rev. 62 (1998) 1046–1078.
[59] E. Arslan, H. Schulz, R. Zufferey, P. Kunzler, L. Thöny-Meyer, Overproduction of the *Bradyrhizobium japonicum c*-type cytochrome subunits of the cbb_3 oxidase in *Escherichia coli*, Biochem. Biophys. Res. Commun. 251 (1998) 744–747.
[60] B. Witholt, M. Boekhout, M. Brock, J. Kingma, H.V. Heerikhuizen, L.D. Leij, An efficient and reproducible procedure for the formation of spheroplasts from variously grown *Escherichia coli*, Anal. Biochem. 74 (1976) 160–170.
[61] J.N. Brønsted, V.K. La Mer, The activity coefficients of ions in very dilute solutions, J. Am. Chem. Soc. 46 (1924) 555–573.
[62] F. Malatesta, The study of bimolecular reactions under non-pseudo-first order conditions, Biophys. Chem. 116 (2005) 251–256.
[63] D. Mooser, O. Maneg, F. Macmillan, F. Malatesta, T. Soulimane, B. Ludwig, The menaquinol-oxidizing cytochrome *bc* complex from *Thermus thermophilus*: protein domains and subunits, Biochim. Biophys. Acta 1757 (2006) 1084–1095.
[64] M.F. Otten, D.M. Stork, W.N. Reijnders, H.V. Westerhoff, R.J. Van Spanning, Regulation of expression of terminal oxidases in *Paracoccus denitrificans*, Eur. J. Biochem. 268 (2001) 2486–2497.
[65] F. Cutruzzolà, M. Arese, M. Brunori, in: A. Messerschmidt, R. Huber (Eds.), Cytochrome c_{551}. Handbook of Metalloproteins, John Wiley & Sons, Ltd, Chichester, 2001, pp. 69–79.
[66] M. Ubbink, M. Ejdeback, B.G. Karlsson, D.S. Bendall, The structure of the complex of plastocyanin and cytochrome *f*, determined by paramagnetic NMR and restrained rigid-body molecular dynamics, Structure 6 (1998) 323–335.
[67] H. Witt, F. Malatesta, F. Nicoletti, M. Brunori, B. Ludwig, Cytochrome-*c*-binding site on cytochrome oxidase in *Paracoccus denitrificans*, Eur. J. Biochem. 251 (1998) 367–373.
[68] G. Engstrom, R. Rajagukguk, A.J. Saunders, C.N. Patel, S. Rajagukguk, T. Merbitz-Zahradnik, K. Xiao, G.J. Pielak, B. Trumpower, C. Yu, L. Yu, B. Durham, F. Millett, Design of a ruthenium-labeled cytochrome *c* derivative to study electron transfer with the cytochrome bc_1 complex, Biochemistry 42 (2003) 2816–2824.
[69] M.I. Verkhovsky, J.E. Morgan, A. Puustinen, M. Wikström, Kinetic trapping in cell respiration, Nature 380 (1996) 268–270.
[70] O. Preisig, R. Zufferey, L. Thöny-Meyer, C.A.H. Appleby, A high affinity cbb_3-type cytochrome oxidase terminates the symbiosis specific respiratory chain of *Bradyrhizobium japonicum*, J. Bacteriol. 178 (1996) 1532–1538.